applied sciences

MDPI

Article

The Use of Rapeseed Husks to Remove Acidic and Basic Dyes from Aquatic Solutions

Tomasz Jóźwiak * and Urszula Filipkowska

Department of Environmental Engineering, University of Warmia and Mazury in Olsztyn, Warszawska St. 117a, 10-957 Olsztyn, Poland; urszula.filipkowska@uwm.edu.pl
* Correspondence: tomasz.jozwiak@uwm.edu.pl

Abstract: This study aimed to identify the possibility of using rapeseed husks (RH) as an unconventional sorbent for removing acidic (AR18, AY23) and basic (BR46, BV10) dyes from aqueous solutions. Its scope included, i.a.: sorbent characterization (FTIR, pH_{PZC}), determination of pH effect on dye sorption effectiveness (pH 2–11), analysis of dye sorption kinetics (pseudo-first order model, pseudo-second order model, intraparticular diffusion model), and the determination of the maximum sorption capacity (Langmuir 1 and 2, and Freundlich isotherms). The sorption effectiveness of acidic dyes (AR18, AY23) onto RH was the highest at pH = 2, whereas that of the basic dyes BR46 and BV10 was most effective at pH = 6 and pH = 3, respectively. The time needed to reach the sorption equilibrium of dyes onto RH depended on their initial concentration and ranged from 120 to 150 min for the acidic dyes and from 150 to 180 min for the basic dyes. The maximum sorption capacity (Q_{max}) of RH towards AR18 and AY23 was 49.37 mg/g and 41.52 mg/g, respectively, and towards BR46 and BV10 it was 59.07 mg/g and 20.93 mg/g, respectively. The obtained Q_{max} values were compared with the results achieved for other sorbents (literature data). This comparison demonstrated that the sorption capacity of rapeseed husks towards the analyzed dyes was higher compared to that of some types of activated carbons.

Keywords: rapeseed husks; hulls; unconventional sorbent; sorption; acidic dyes; basic dyes; Acid Red 18; Acid Yellow 23; Basic Red 46; Basic Violet 10

Citation: Jóźwiak, T.; Filipkowska, U. The Use of Rapeseed Husks to Remove Acidic and Basic Dyes from Aquatic Solutions. *Appl. Sci.* **2024**, *14*, 1174. https://doi.org/10.3390/app14031174

Academic Editor: Dino Musmarra

Received: 20 December 2023
Revised: 25 January 2024
Accepted: 29 January 2024
Published: 30 January 2024

1. Introduction

Dyes are chemical compounds used to impart a desired color to utility items. There are about 10,000 types of dyes available on the market and their global production currently exceeds 1 million ton/year [1]. They are mainly used in industry for dyeing fibers, leather, plastics, paper, foods, and other materials. As a result of certain drawbacks of the dyeing technology, a significant proportion of the dyes used is lost and ends up in wastewater [2].

Colored industrial wastewater poses a serious risk to the natural environment. For example, ineffective methods of decolorization of post-production waters cause certain amounts of dyes to pervade the natural waters [3]. Furthermore, even small amounts of color substances can trigger major changes in local aquatic ecosystems [4]. Most dyes are very visible in water reservoirs, even at concentrations of 1 mg/L, which disturbs the aesthetics of the latter [5]. What is worse, they impair sunlight penetration through water, thus, inhibiting the photosynthesis carried out by aquatic autotrophs [6]. In addition, some dyes hinder the diffusion of atmospheric oxygen in water, which, when combined with impaired photosynthesis, can lead to the development of anaerobic conditions in the water reservoir. Certain dyes may also be toxic to aquatic organisms [7]. As a result, pollution with dyes can lead to the collapse of the local aquatic ecosystem. In order to minimize the risk of environmental degradation, it seems necessary to implement effective technologies for wastewater decolorization.

Colored wastewater is most often treated by means of physicochemical methods including: chemical precipitation and electrocoagulation, chemical oxidation methods (e.g.,

ozonation or reaction with sodium hypochlorite), membrane methods (e.g., ultrafiltration, reverse osmosis), and also sorption methods [8,9]. Sorption involves binding contaminants on the surface of the material (sorbent). Unlike precipitation or deep oxidation methods, it does not generate any by-products [10]. Sorption methods are also easier to carry out and are cheaper compared to the membrane methods.

Many scientists are of the opinion that dye sorption is one of the safest methods for wastewater decolorization [11]. The effectiveness and costs of colored wastewater treatment by means of sorption depend mainly on the type of sorbent used. Currently, sorbents that are most commonly used for water and wastewater treatment include activated carbon-based materials [12]. They are characterized by high porosity and very extensive specific surface area, often exceeding 1000 m^2/g, which translates into their good sorption of most dyes [13]. The main problems associated with activated carbons include their rapid saturation, difficult regeneration and the associated weight loss. There is also a common opinion that their production costs are high. Therefore, their cheaper alternatives are currently being sought. They should be readily available, cheap and, possibly, have a sorption capacity similar to that of activated carbons. Today, high hopes are fostered in waste materials from the agri-food industry as either sorbents or raw materials for their production [14,15]. They are cheap and widely available, especially in developed countries. So far, research has been carried out on the removal of dyes on waste materials from the agricultural industry such as plant stalks, leaves, nut shells or fruit skins [16,17]. Their sorption capacity is mainly due to the high contents of polysaccharides, lignin and proteins.

An example of a widely available waste material from the agri-food industry with potentially good sorption capacity is rapeseed husks. Rape (*Brassica napus* L.) is one of the most popular crops. In 2020, its global production exceeded 70 million tons [18]. It is grown mainly for seeds containing 40–45% fat [19,20] that are used for oil production for food purposes or for biodiesel production [21]. The residue from the oil pressing is the so-called rapeseed oil cake, containing the husk and crushed seed kernel. It is usually used as an additive to animal feedstuffs. Seed husks, which account for approximately 20% of rape seed weight [22], can be easily isolated from rapeseed cake. They consist of polysaccharides (cellulose, hemicellulose)—33%; lignin—26%; and proteins—18% [23,24], which may suggest their potentially high usability in removing both acidic and basic dyes from aqueous solutions.

This study examined the possibility of using rapeseed husks as an unconventional sorbent to remove dyes from aqueous solutions. To this end, sorption capacity of rapeseed husks was tested in respect of acidic dyes (Acid Red 18, Acid Yellow 23) and basic dyes (Basic Red 46, Basic Violet 10) popular in the industry.

2. Materials and Methods

2.1. Rapeseed Husks

The raw material used to prepare the sorbent consisted of rapeseed oil cake supplied by an oil extrusion plant located in the Warmińsko-Mazurskie Province (Poland). The cake derived from industrial rape seeds from the local harvest of 2022.

The sorbent preparation consisted in separating the husks from the crushed rape seed kernel (acc. to the procedure described in Section 2.5). Rape seed husks (RH) accounted for 31% of the oil cake weight. The content of individual components in the husk dry matter was as follows: lignin—25.0%; cellulose—13.7%; hemicellulose—19.0%; pectin—12.0%; proteins—18.1%; starch—0.4%; and other components (e.g., lipids, monosugars, ash)—12.2% [23,24].

2.2. Sorb—Ates (Dyes)

Acidic dyes: Acid Red 18 (AR18) and Acid Yellow 23 (AY23); and basic dyes: Basic Red 46 (BR46) and Basic Violet 10 (BV10), were purchased at the Dye-Producing Industry Plant "BORUTA-ZACHEM KOLOR SA" in Zgierz (Poland). Table 1 presents the key parameters of dyes provided by the producer.

Table 1. Characteristics of dyes used in the study.

Dye Name	Acid Red 18 (AR18)	Acid Yellow 23 (AY23)	Basic Red 46 (BR46)	Basic Violet 10 (BV10) (BV10)
Structural formula	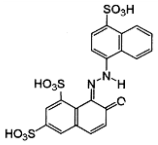	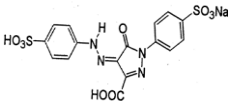	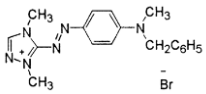	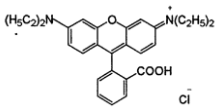
Chemical formula	$C_{20}H_{11}N_2Na_3O_{10}S_3$	$C_{16}H_9N_4Na_3O_9S_2$	$C_{18}H_{21}BrN_6$	$C_{28}H_{31}ClN_2O_3$
Molecular weight	604.5 g/mol	534.4 g/mol	321.4 g/mol	479.0 g/mol
Dye class	single azo dye	single azo dye	single azo dye	xanthene dye
Dye type	anionic (acidic)	anionic (acidic)	cationic (basic)	cationic (basic)
λ_{max}	509 nm	428 nm	530 nm	554 nm
Uses	dyeing wool, silk, polyamide fiber	dyeing wool, silk, polyamide fiber	dyeing leather, paper, wool, and acrylic fibers	dyeing textiles, paper, leather
Hazards	may cause irritation; may be harmful if swallowed	may cause skin irritation, may cause gastrointestinal irritation	caustic, toxic, hazardous to the aquatic environment	toxic, fluorescent, carcinogenic; can induce skin and eye allergies
Other trade names	Acid Brilliant Red 3R, Acid Scarlet 3R, Red 3R	Tartrazine, Acid Tartrazine, Aizen Tartrazine	Anilan Red GRL, Basic Red X-GRL, Cationic Red X-GRL	Rhodamine B, Basic Red RB, Violet B.
Dye content in the commercial product	75%	85%	80%	80%

2.3. Chemical Reagents

- Hydrochloric acid (HCl)—37%—(solution pH correction),
- Sodium hydroxide (NaOH) > 99.9%—micropellets—(solution pH correction),

All chemical reagents used were purchased from POCH S.A., Gliwice, Poland, and were of p.a. (analytical purity) grade or higher.

2.4. Laboratory Equipment

- FT/IR-4700LE FT-IR Spectrometer with a single reflection ATR attachment (JASCO International, Tokyo, Japan)—for preparing the sorbent's FTIR spectra;
- UV-3100 PC—UV/Visible spectrophotometer (VWR spectrophotometers, VWR International LLC., Mississauga, ON, Canada)—for determining the concentration of dye in solutions;
- HI 221 pH-meter (Hanna Instruments, Woonsocket, RI, USA)—for the measurement and correction of the solutions pH;
- Multi-Channel Stirrer MS-53M (JEIO TECH, Daejeon, Republic of Korea)—for the process of sorption;
- Gemini VI (Micromeritics, Norcross, GA, USA)—for the measurements of porosity and surface area of the sorbent.

2.5. Sorbent Preparation—Rape Seed Husks (RH)

The rapeseed cake was placed in a laboratory beaker that was filled up with hot deionized water (50–55 °C). The contents of the beaker were mixed for 5 min with a spatula. During mixing, the crushed kernels of the rapeseed were separated from the husks. The contents of the beaker were then poured through a laboratory sieve with a mesh diameter of 0.5 mm. This mesh size ensured that the husks were retained on the sieve while allowing the crushed kernels of rapeseed to pass through. The husks that had remained on the

sieve (mesh size 0.5–2.5 mm) were reintroduced into the beaker to repeat the process of separating the seed nucleus from the husks (washing the husks). The process was repeated many times until the water after husk washing was clear (without turbidity caused by the crushed kernel), and the husks drained on the sieve were completely devoid of the nucleus. Afterwards, the husks were dried in a laboratory drier at a temperature of 105 °C. The ready-to-test sorption material in the form of purified and dried rape seed husks (RH) was stored in a sealed polypropylene container.

2.6. Analyses of pH Effect on Dye Sorption Effectiveness

For pH effect analysis, 2.5 g portions of RH were weighed using a precision scale to a series of beakers (600 mL). Dye solutions (500 mL) with a concentration of 50 mg/L and pH between 2 and 11 were then added to the beakers. Next, the beakers were placed on a multi-station magnetic stirrer (200 r.p.m.) for 120 min. Standard magnetic stirrers with a Teflon coating (50 × 8 mm in size) were used for mixing the contents of the beakers. After the allotted time, samples of the solutions were taken with an automatic pipette (10 mL) into the earlier prepared polypropylene tubes. The pH value of the solutions was also measured after the sorption process.

2.7. Analyses of Dye Sorption Kinetics

For dye sorption kinetics analysis, 5.0 g portions of RH were measured using a precision scale into beakers (2500 mL). Afterwards, dye solutions (2000 mL) having the following concentrations: 50/100/250 mg/L in the case of AR18, AY23, BR46 dyes or 20/50/100 mg/L in the case of BV10 dye, and optimal pH (established during analyses described in Section 2.6) were added to the beakers. The beakers were then placed on a multi-station magnetic stirrer (200 r.p.m., a stirrer of 80 × 10 mm in size). After allotted periods of time (0, 10, 20, 30, 45, 60, 90, 120, 150, 180, 210, 240, and 240 min), 5-mL samples of the solutions were collected with an automatic pipette to the earlier prepared test tubes.

2.8. Analyses of the Maximum Sorption Capacity of RH

The sorbent (RH) was weighed in 2.5 g portions into a series of beakers (600 mL). Next, dye solutions (500 mL) having the following concentrations: 10–500 mg/L in the case of AR18, AY23, BR46 dyes or 2–250 mg/L in the case of BV10 dye, and optimal pH (established during analyses described in Section 2.6), were added to the beakers. The flasks were then placed on a multi-station magnetic stirrer (200 r.p.m., 50 × 8 mm in size) for the time needed to reach sorption equilibrium (established based on analyses performed as described in Section 2.7). Afterwards, 10 mL samples of dye solutions were collected from the beakers to the earlier prepared test tubes.

In all experimental series (Sections 2.6–2.8), the mixing speed and the size of the stirrer ensured even distribution of the sorbent (RH) throughout the dye solution's volume. In each experiment, dye solutions had a temperature (25 °C). The concentration of the dye remaining in the solution was determined with the spectrophotometric method using a UV-VIS spectrophotometer. The lower dye concentrations determined in the experimental series with BV10 (Sections 2.7 and 2.8) were due to a noticeably inferior RH sorption capacity of this dye. All experimental series were performed in three replications.

2.9. Computation Methods

The amount of dye adsorbed on RH was determined from formula (1).

$$Qs = (C_0 - C_S) \times \frac{V}{m} \quad (1)$$

Q_S—mass of sorbed dye [mg/g]
C_0—initial concentration of dye [mg/L]
C_S—concentration of dye after sorption [mg/L]
V—volume of the solution [L]

m—mass of the sorbent [g].

The kinetics of dye sorption onto RH was described using the pseudo-first order model (2), the pseudo-second order model (3), and the intraparticular diffusion model (4).

$$Q = q_e \times \left(1 - e^{(-k_1 \times t)}\right) \tag{2}$$

$$Q = \frac{(k_2 \times {q_e}^2 \times t)}{(1 + k_2 \times q_e \times t)} \tag{3}$$

$$Q = k_{id} \times t^{0.5} \tag{4}$$

Q—instantaneous value of the sorbed dye [mg/g]
q_e—the amount of dye sorbed at the equilibrium state [mg/g]
t—time of sorption [min]
k_1—pseudo-first order adsorption rate constant [1/min]
k_2—pseudo-second order adsorption rate constant [g/(mg·min)]
k_{id}—intraparticular diffusion model adsorption rate constant [mg/(g·min$^{0.5}$)].

The experimental data obtained from studies on the maximum sorption capacity of RH were described using three popular sorption models: the Langmuir 1 isotherm (5), the Langmuir 2 isotherm (Langmuir double isotherm) (6), and the Freundlich isotherm (7). The Langmuir 2 isotherm, also known as the "dual-site Langmuir model", describes the adsorption of one type of sorbate on two types of sorption centers. It allows each active site to be described with a separate Langmuir equation [25].

$$Qs = \frac{(Q_{max} \times K_C \times C)}{(1 + K_C \times C)} \tag{5}$$

$$Qs = \frac{(b_1 \times K_1 \times C)}{(1 + K_1 \times C)} + \frac{(b_2 \times K_2 \times C)}{(1 + K_2 \times C)} \tag{6}$$

$$Qs = K \times C^{\frac{1}{n}} \tag{7}$$

Qs—mass of the sorbed dye [mg/g]
Q_{max}—maximum sorption capacity in Langmuir equation [mg/g]
b_1—maximum sorption capacity of sorbent (type I active sites) [mg/g]
b_2—maximum sorption capacity of sorbent (type II active sites) [mg/g]
K_C—constant in Langmuir equation [L/mg]
K_1, K_2—constants in Langmuir 2 equation [L/mg]
K—the equilibrium sorption constant in Freundlich model
n—Freundlich equilibrium constant
C—concentration of dye remaining in the solution [mg/L]
n—constant in the Freundlich model.

3. Results and Discussion

3.1. Characteristics of RH (FTIR, Surface)

The FTIR spectrum of rapeseed husks (Figure 1) was typical of the lignocellulosic plant biomass. Peaks in the range of 1400–900 cm^{-1} were characteristic for bonds and functional groups of polysaccharides present in the material [26]. The peaks visible at 1024 cm^{-1}; 1048 cm^{-1}; 1144 cm^{-1}; and also 1201 cm^{-1} may be ascribed to the C-O-C bond found in the aromatic rings of cellulose and hemicellulose [27]. In turn, peaks at 956 cm^{-1} and 896 cm^{-1} indicate the bending of the C-O-H bond of β-glucans [28]. The absorption bands at 1420 cm^{-1} and 1371 cm^{-1} correspond to the tensile and bending vibrations of -CH_2 bonds of cellulose [29]. The presence of lignin in the analyzed material may be indicated by a peak visible at 1236 cm^{-1} corresponding to the C=C bond of the guaiacol aromatic ring and also a peak at 1316 cm^{-1} assigned to the stretching of the C-O bond of the syringyl ring [30].

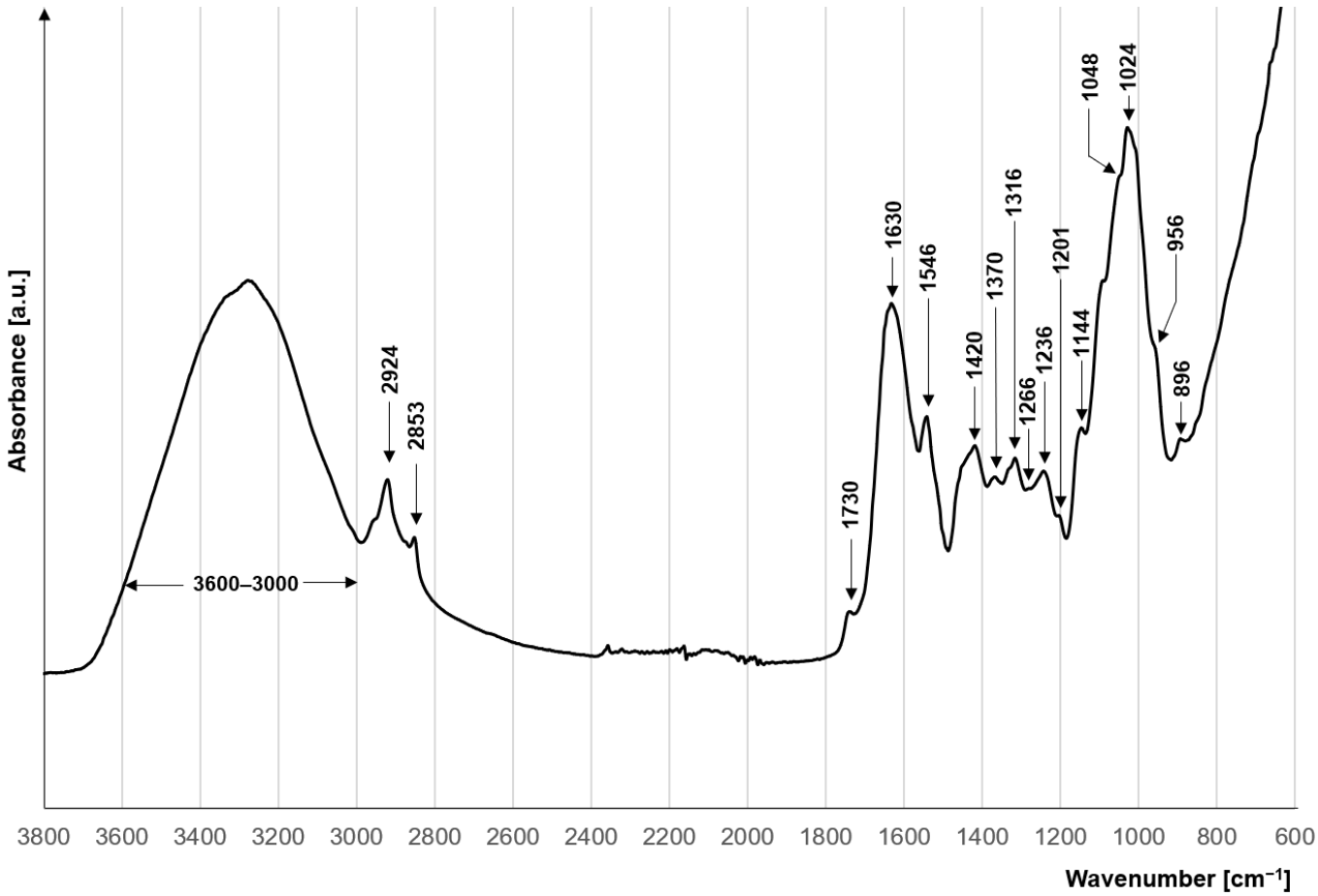

Figure 1. FTIR spectra of rapeseed husks (RH).

A wide band noticeable at 3500–3000 cm^{-1} denotes the stretching of the O-H bond of hydroxyl functional groups. The peak visible in this band at 3278 cm^{-1} corresponds to the symmetrical stretching of the N–H bond (amide A) of biomass proteins [31]. The protein content of rapeseed husks may also be indicated by peaks visible at 1546 cm^{-1} and 1266 cm^{-1}, which are ascribed to N–H bonds of secondary and tertiary amides [32]. A distinct peak visible at 1630 cm^{-1} indicates the presence of carboxylic groups in the analyzed material [33]. In turn, the absorption band at 1730 cm^{-1} is attributed to the carbonyl group C=O of the ester bond, which may be related to the content of fatty acids, glycerides, and pectins in rapeseed husks [34]. Peaks at 2924 cm^{-1} and 2853 cm^{-1} correspond to asymmetric and symmetrical stretching vibrations of the -CH_2- group, which may belong to lipid chains or terminal protein groups [34,35].

The specific surface area and RH porosity were measured using the Gemini VI apparatus from Micromeritics. The BET area determined for rapeseed husks was 1064 m^2/g, whereas the total pore volume determined for RH was 0.00223 cm^3/g.

3.2. The Effect of pH on the Effectiveness of Dye Sorption onto RH

The sorption effectiveness of acidic dyes (AR18, AY23) onto RH was the highest at pH = 2 and decreased along with pH increasing up to pH = 11. The greatest decrease in the binding effectiveness of these dyes onto the tested sorbent was recorded in the pH range of 2–4. In the pH range, of pH 5–10, the AR18 and AY23 sorption effectiveness onto RH was similar and low (Figure 2a).

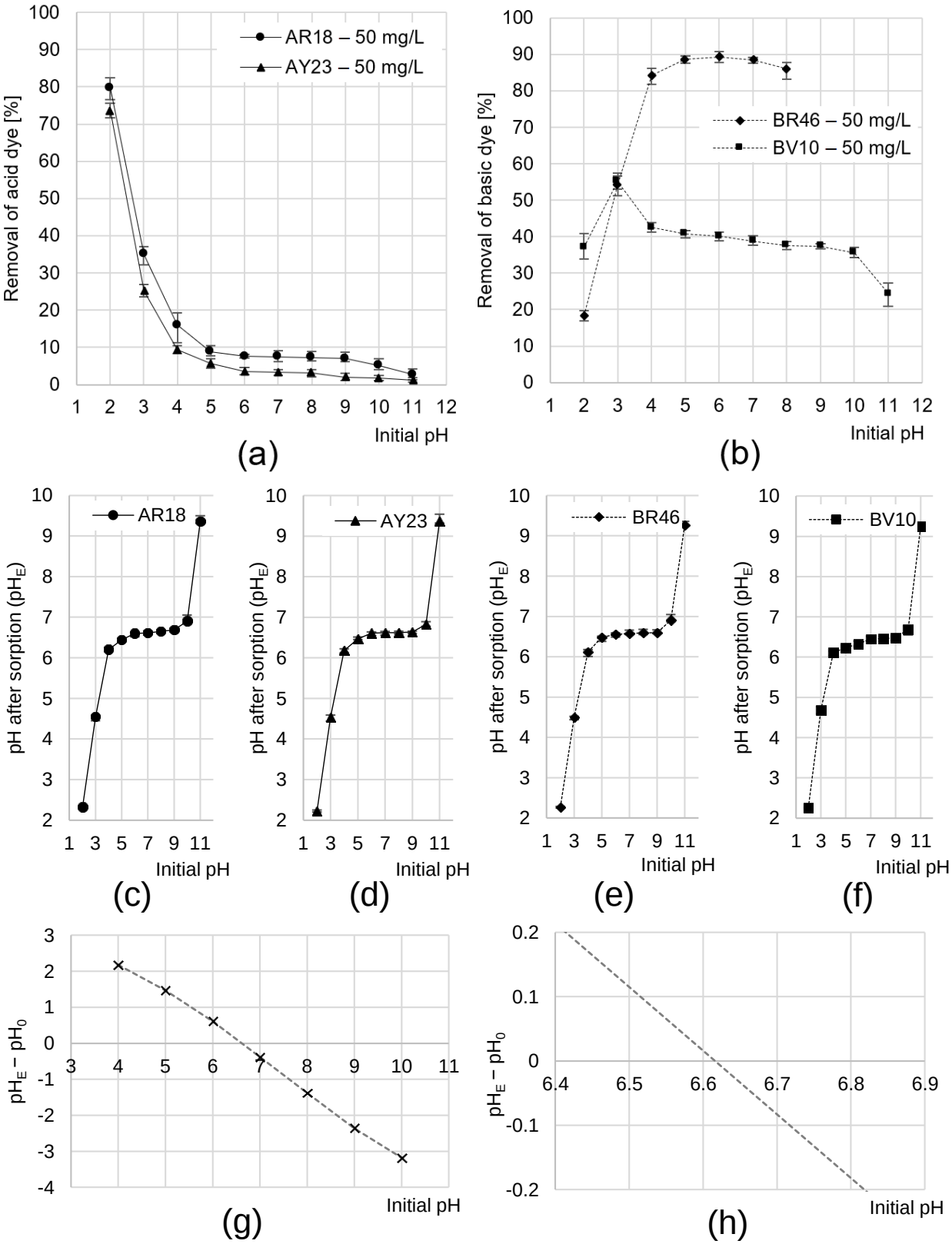

Figure 2. Effect of pH on the effectiveness of sorption of (**a**) acidic dyes (AR18/AY23) and (**b**) basic dyes (BR46/BV10) onto RH (average + range). Effect of RH on changes in solution pH after sorption of (**c**) AR18, (**d**) AY23, (**e**) BR46, and (**f**) BV10. (**g**,**h**) Determination of pH_{PZC} of the RH using the "drift" method.

The high sorption effectiveness of anionic dyes on RH in the acidic environment might have been due to the positive charge gained by sorbent's surface. At pH < 6, most of the amine groups [36] underwent protonation, whereas the hydroxyl groups started to undergo protonation presumably at pH < 3.

$$\text{-OH} + H_3O^+ \rightarrow \text{-}OH_2^+ + H_2O$$

$$\text{-}NH_2 + H_3O^+ \rightarrow \text{-}NH_3^+ + H_2O$$

Positively charged RH functional groups attracted electrostatically the ionized sulfone groups of AR18 and AY23, which significantly intensified their sorption. Since the number of protonated functional groups increased with pH decrease, the highest binding effectiveness was obtained at the lowest pH tested (pH = 2).

Rapeseed husks have a high content of polysaccharides (cellulose, hemicellulose) and lignin (rich in hydroxyl groups) and a fairly low content of proteins (having amine groups). Due to the low content of the amine groups (despite their high ionization susceptibility at pH < 6), the total number of functional groups protonated on the RH surface in the pH range of 4–6 was relatively low, which explains the low sorption effectiveness of AR18 and AY23 in this pH range.

In an alkaline environment, the sorbent's surface might have gained a negative charge, presumably due to deprotonation of certain functional groups (e.g., hydroxyl ones).

$$\text{-OH} + OH^- \rightarrow \text{-}O^- + H_2O$$

A negatively charged RH surface could repel the dyes electrostatically.

With the increase in pH, the number of deprotonated functional groups of RH increased, which translated into an increasing total negative charge of the sorbent and, thus, a stronger inhibition of dye sorption. This explains the lowest sorption effectiveness of both AR18 and AY23 determined at pH = 11.

The high sorption effectiveness of AR18 at low pH was also noted in the studies addressing the treatment of colored aquatic solutions on sunflower husks [37], chitosan flakes [38], and also activated carbons [39]. In the case of AY23, the positive effect of low pH was also observed during decolorization of solutions on sawdust [40] and chitin [41].

The sorption effectiveness of the cationic dye BR46 onto RH increased with pH increasing up to pH = 6 (Figure 2b). The greatest leap in the binding effectiveness of this dye on the tested sorbent was noted in the pH range of 2–4. At pH > 7, the sorption effectiveness of BR46 on rapeseed husks was observed to decrease (Figure 2b). Due to the spontaneous decolorization of BR46 solutions at pH > 8, the results related to its sorption in the pH range of 9–11 are not presented in Figure 2b.

The relatively high effectiveness of basic BR46 sorption onto rapeseed husks over a broad pH range (pH 4–8) may be due to the generally acidic nature of the sorbent. Ionized carboxyl groups located on RH surface can serve as sorption centers for BR46. The binding of BR46 on the analyzed sorbent can also proceed through hydrogen bonds (between hydrogen and nitrogen atoms, and between hydrogen and oxygen) and Van der Waals forces.

The low sorption effectiveness of BR46 at low pH (pH = 2) was due to a strong positive charge on the surface of the sorbent, which electrostatically repelled BR46 cations. With the increase in pH, the number of protonated functional groups of RH decreased. At pH = 6, their number was already very low, thanks to which BR46 sorption was not impaired by electrostatic interactions with the sorbent's surface.

Despite the cationic nature of BR46, the pH increase above pH = 7 had no positive effect on its binding onto RH (Figure 2b), presumably due to the increasing concentration of Na^+ cations, which competed with dye cations for free sorption centers.

A similar effect of pH on the BR46 sorption effectiveness has also been noted in studies on the decolorization of aqueous solutions using citrus peel [42], crop leaves [43] and granular activated carbons [44].

The effectiveness of BV10 sorption onto the analyzed sorbent was the highest at pH = 3 and decreased along with pH increase. A significant decrease in its binding effectiveness was also noted when the pH dropped from pH = 3 to pH = 2 in the system (Figure 2b).

A characteristic feature of the BV10 dye is its carboxyl functional group. Being capable of easy ionization, it is able to generate a local negative charge in the dye molecule. Owing to this property, BV10 can behave like an anionic dye in sorption systems despite its generally cationic nature. This explains the—unusual for the alkaline dye—effect of pH on its sorption effectiveness, i.e., sorption effectiveness increase along with solution pH decrease (Figure 2b).

A noticeable decrease in the binding effectiveness of BV10 at pH drop from pH = 3 to pH = 2 may be due to deionization of the carboxyl group of the dye. The loss of the local negative charge in the dye's molecule significantly weakened the electrostatic interactions with the positively charged surface of RH.

A very similar effect of pH on the BV10 sorption effectiveness, manifested by the highest intensity noted at pH = 3, has also been demonstrated in studies addressing the sorption properties of spent tea leaves [45], mealworm molts [46], and activated carbon from palm bark [47].

Rapeseed husks had a significant effect on the solution's pH change during sorption (Figure 2c–f). In the case of the solutions with the initial pH of 4–10, their post-sorption pH was set within the range of 6.12–6.90, which was due to the material having easily ionizable alkaline and acidic functional groups.

Alkaline groups (e.g., amino groups) started to undergo protonation at pH < 9. In an acidic environment, they took protons from hydronium ions, whereas in a neutral or slightly alkaline environment—from water molecules. In each case, this increased the pH in the system.

$$\text{-}NH_2 + H_3O^+ \rightarrow \text{-}NH_{3+} + H_2O^{-}(\text{pH increase in the acidic environment})$$
$$\text{-}NH_2 + H_2O \rightarrow \text{-}NH_{3+} + OH^{--}(\text{pH increase in the neutral and slightly alkaline environment}).$$

In turn, acidic functional groups, like carboxylic groups, were deprotonated already at pH > 3. The proton released by the functional group attached itself to a hydroxyl ion (in the alkaline environment) or to a water molecule (in the neutral or acidic environment), causing solution's pH to decrease.

$$\text{-}COOH_2 + OH^- \rightarrow \text{-}COO^- + H_2O^{-}(\text{pH decrease in the acidic environment})$$
$$\text{-}COOH + H_2O \rightarrow \text{-}COO^- + H_3O^{-}(\text{pH reduction in the neutral and slightly acidic environment})$$

The nature of pH change in the solution depends mainly on the ratio of alkaline groups to acidic groups on the surface of the sorption material. For this reason, the system always tends to reach the pH value that is close to the pH_{PZC} (the point of zero charge) of the sorbent. The PZC determined for RH with the drift method was pH_{PZC} = 6.62. (Figure 2g,h). This suggests the slightly acidic nature of the sorbent, which may be induced by a higher number of carboxylic groups than amine groups on its surface.

Further stages of the study described in Sections 3.3 and 3.4 were accomplished at the optimal sorption pH, which was pH = 2 for the acidic dyes (AR18, AY23) as well as pH = 6 and pH = 3 for the basic dyes (BR46 and BV10, respectively).

3.3. The Kinetics of Dye Sorption onto RH

The time needed to reach sorption equilibrium for the acidic dyes on RH depended on their initial concentration and ranged from 120 min for their concentration of 250 mg/L to 150 min for their concentrations of 50–100 mg/L (Figure 3a,b, Table 2). The sorption intensity of AR18 and AY23 dyes on the tested material was the highest in the initial stage of the process. After 20 min, the amount of the sorbent-bound AR18 ranged from 59 to 72% of q_e and that of AY23 from 65 to 75% of q_e.

A similar sorption equilibrium time has also been noted in studies on the sorption of AR18 on cellulose flakes (120 min) [38] and activated carbon from poplar wood

(120 min) [48]. In the case of AY23, a similar equilibrium time was obtained in experiments determining its removal on chitin flakes (120 min) [41] as well as activated carbon from coconut coir (120 min) [49].

The sorption time of cationic dyes on the analyzed sorbent ranged from 150 min for their higher concentrations (250 mg BR46/L/100 mg BV10/L) to 180 min for their lower concentrations (50–100 mg BR46/L/20–50 mg BV10/L) (Figure 3c,d). As with acidic dyes, the binding intensity of BR46 and BV10 onto RH was highest in the first minutes of the process. In the experimental series with BR46, after 20 min of sorption, the amount of dye bound to RH was 63–68% of q_e and that of BV10 was 58–64% of q_e.

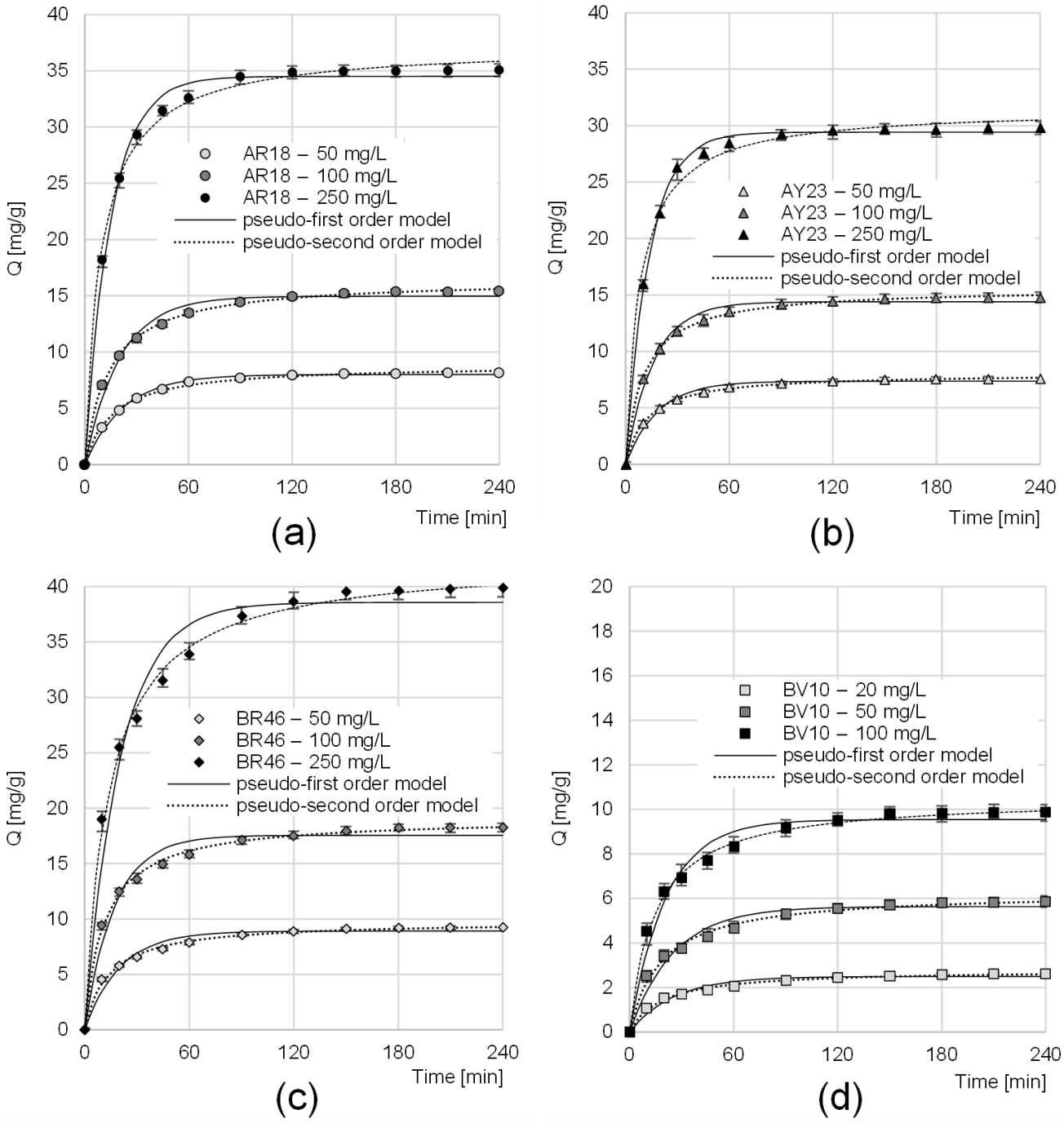

Figure 3. Sorption kinetics of (**a**) AR18, (**b**) AY23, (**c**) BR46, and (**d**) BV10 onto RH (average + range). Pseudo-first-order model and pseudo-second-order model.

Table 2. Kinetic parameters of the sorption of dyes onto RH determined from the pseudo-first order and pseudo-second order models. Constants determined based on mean values from three measurements.

Dye	Dye Conc.	Pseudo-First Order Model			Pseudo-Second Order Model			Exp. Data	Equilibrium Time
	[mg/L]	k_1 [1/min]	$q_{e,cal.}$ [mg/g]	R^2 -	k_2 [g/mg·min]	$q_{e,cal.}$ [mg/g]	R^2 -	$q_{e,exp.}$ [mg/g]	[min]
AR18	50	0.0453	8.01	0.9953	0.0072	8.89	0.9964	8.14	150
	100	0.0497	14.97	0.9846	0.0044	16.48	0.9993	15.41	150
	250	0.0670	34.50	0.9942	0.0029	37.20	0.9965	35.07	120
AY23	50	0.0548	7.37	0.9883	0.0103	8.06	0.9992	7.56	150
	100	0.0621	14.40	0.9889	0.0062	15.62	0.9992	14.77	150
	250	0.0733	29.44	0.9759	0.0039	31.55	0.9922	29.82	120
BR46	50	0.0497	8.91	0.9704	0.0075	9.80	0.9964	9.24	180
	100	0.0586	17.55	0.9721	0.0047	19.13	0.9979	18.27	180
	250	0.0492	38.59	0.9732	0.0017	42.47	0.9968	39.89	150
BV10	20	0.0396	2.49	0.9663	0.0194	2.80	0.9944	2.61	180
	50	0.0396	5.63	0.9675	0.0088	6.30	0.9936	5.85	180
	100	0.0478	9.54	0.9738	0.0066	10.54	0.9971	9.87	150

A similar sorption equilibrium time was also observed in the studies analyzing BR46 sorption onto sawdust (120 min) [50], coconut shells (120 min) [51], as well as mealworm molts (150 min) [46] and mealworm exoskeletons (180 min) [46]. In the case of BV10, a comparable sorption equilibrium time was recorded in the experiments on its binding on carbonized coconut fibers (150 min) [52], and spent coffee grains (180 min) [53].

In general, shorter sorption times achieved at the higher initial concentrations of dyes may be due to a higher probability of dye particle collisions with sorbent sorption centers. Faster saturation of active RH sites resulted in faster reaction completion.

The longer sorption times of the alkaline dyes onto RH, compared to the acidic dyes, may have been the result of their higher molecular weight (AR18—604.5 g/mol; AY23—534.4 g/mol vs. BR46—321.4 g/mol; BV10—479.0 g/mol). The smaller particle sizes of the BR46 and BV10 dyes could theoretically allow them to reach the sorption centers in deeper sorbent's layers inaccessible to AR18 and AY23. However, the migration of basic dye molecules to the active sites located in hardly accessible sites required a relatively large amount of time. In the case of AR18 and AY23, the dye molecules were likely to quickly clog the entries to RH pores, which blocked the access to functional groups located in deeper sorbent's layers and could speed up sorption completion.

Experimental data from studies on the kinetics of dye sorption onto RH were described with the pseudo-first order and pseudo-second order models. In each experimental series, the pseudo-secondary model showed the best fit to experimental data, regardless of the initial dye concentration (Figure 3, Table 2).

The values of k_2 constant and q_e determined from the model indicate that for each tested dye, the intensity of its sorption onto RH increased along with the increase in its initial concentration. The strong correlation between dye concentrations and sorption rate constants may indicate a rather weak affinity of the functional groups of dyes to the active sites of the sorbent.

The sorption kinetics of the analyzed anionic dyes AR18 and AY23 was similar, which could be due to the same nature of the dyes, their similar molar mass and the same number of their acidic functional groups. The lower sorption effectiveness of the basic dye BV10 onto RH compared to the BR46 dye may have been caused by the different pHs applied during sorption as well as by the carboxyl functional group present in dye's structure, which is untypical of the acidic dyes.

The sorption of dyes onto RH was also described using the intraparticular diffusion model (Table 3, Figure 4). Graphs plotted from the obtained experimental data suggest that dye sorption onto the tested sorbent proceeded in three main phases. In the first, most intense but relatively short phase, the dye molecules diffused from the solution to the sorbent's area and occupied the most accessible active sites on the RH surface.

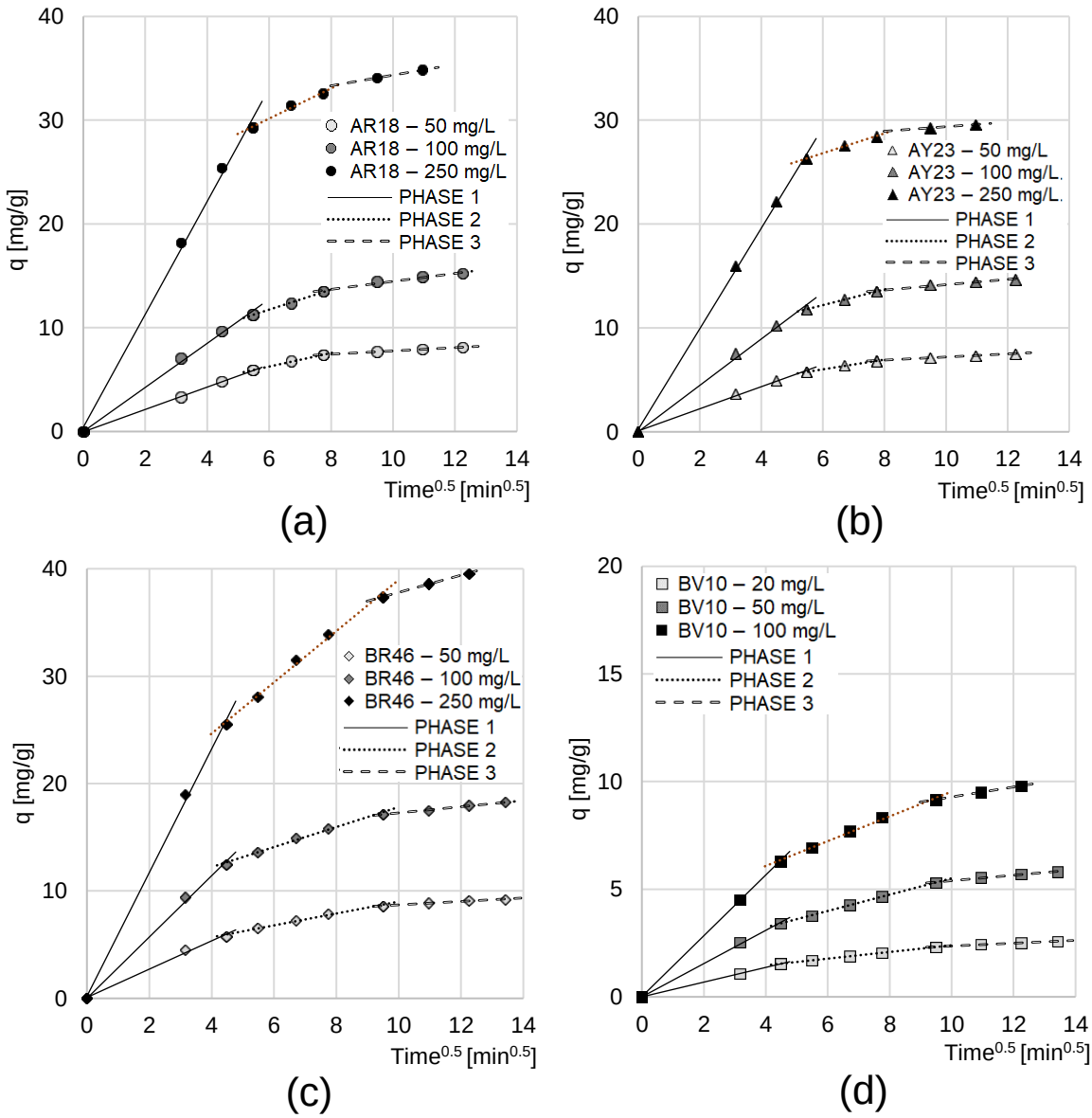

Figure 4. Intraparticular diffusion model of the sorption of: (**a**) AR18, (**b**) AY23, (**c**) BR46, and (**d**) BV10 onto RH (average + range).

When most sorption centers had been saturated on the sorbent's surface, phase two began. In this phase, the dye molecules probably began to occupy active sites located in more difficult-to-reach sites of RH, such as pores. This phase was characterized by great competition between dye molecules for free active centers, which, when combined with a small number of active sites, translated into a lower sorption intensity. When most sorbent's sorption centers had been saturated with dye particles, phase three began—the least intense and the longest in most cases. It consisted in the slow saturation of the last active sites in the pores of RH [54]. After the third phase, the systems entered into a state of sorption equilibrium.

Table 3. Dye diffusion rate constants, determined from the intraparticular diffusion model. * [mg/(g·min$^{0.5}$)] Constants determined based on mean values from three measurements.

Dye	Dye Conc. [mg/L]	Phase I			Phase II			Phase III		
		k_{d1} * [*]	Durat. [min]	R^2 -	k_{d2} * [*]	Durat. [min]	R^2 -	k_{d3} * [*]	Durat. [min]	R^2 -
AR18	50	1.076	30	0.9996	0.655	30	0.9975	0.161	90	0.9913
	100	2.122	30	0.9990	0.967	30	0.9969	0.385	90	0.9567
	250	5.444	30	0.9964	1.458	30	0.9837	0.520	60	0.(9)
AY23	50	1.066	30	0.9964	0.469	30	0.9990	0.150	90	0.9866
	100	2.238	30	0.9983	0.752	30	0.9993	0.253	90	0.9504
	250	4.849	30	0.9973	0.951	30	0.9973	0.222	60	0.(9)
BR46	50	1.319	20	0.9931	0.555	70	0.9846	0.164	90	0.9718
	100	2.854	20	0.9990	0.932	70	0.9907	0.285	90	0.9959
	250	5.758	20	0.9983	2.386	70	0.9939	0.799	60	0.9949
BV10	20	0.342	20	0.9999	0.155	70	0.9966	0.065	90	0.9801
	50	0.774	20	0.9996	0.382	70	0.9994	0.126	90	0.9822
	100	1.412	20	0.9998	0.575	70	0.9959	0.233	60	0.9996

The values of k_{d1}, k_{d2} and k_{d3} constants determined from the intraparticular diffusion model correlated strongly with the initial dye concentration. This confirms the relatively low affinity of the tested dyes to the RH functional groups. The longer duration of the first sorption phase of basic dyes compared to the acidic dyes could be due to the very strong electrostatic interaction of the negatively charged functional groups of AR18 and AY23 with the positively charged RH surface at pH = 2. In the second phase, when RH pores were saturated with dye molecules, the alkaline dyes already had a clear advantage over the acidic dyes due to their smaller particle sizes. This was mainly manifested in the longer duration of this phase.

3.4. Maximum Sorption Capacity of RH

Experimental data obtained from studies into the maximum sorption capacity were described with popular sorption models: Langmuir 1 isotherm, Langmuir 2 isotherm, and Freundlich isotherm (Table 4, Figure 5). An analysis of the values of R^2 determination coefficient shows that the Langmuir models better fitted to the data than the Freundlich's model in each experimental series. This suggests that only one molecule of dye could be attached to one RH active site. In addition, the adsorbed dyes formed the so-called monolayer on the sorbent's surface, where the dyes could exchange their sorption centers among each other.

Table 4. Constants determined from Langmuir 1, Langmuir 2, and Freundlich models (constants determined based on mean values from three measurements).

Dye	Langmuir 1 Model			Langmuir 2 Model						Freundlich Model		
	Q_{max} [mg/g]	K_c [L/mg]	R^2 -	Q_{max} [mg/g]	b_1 [mg/g]	K_1 [L/mg]	b_2 [mg/g]	K_2 [L/mg]	R^2 -	k -	n -	R^2 -
AR18	49.37	0.0271	0.9895	49.37	23.60	0.0271	25.77	0.0271	0.9895	5.754	0.375	0.8970
AY23	41.52	0.0231	0.9894	41.52	20.76	0.0231	20.76	0.0231	0.9894	4.511	0.378	0.9054
BR46	55.59	0.0529	0.9986	59.07	12.22	0.0086	46.85	0.0665	0.9993	9.209	0.337	0.9155
BV10	19.78	0.0209	0.9995	20.93	10.08	0.0329	10.85	0.0106	0.9997	1.314	0.493	0.9793

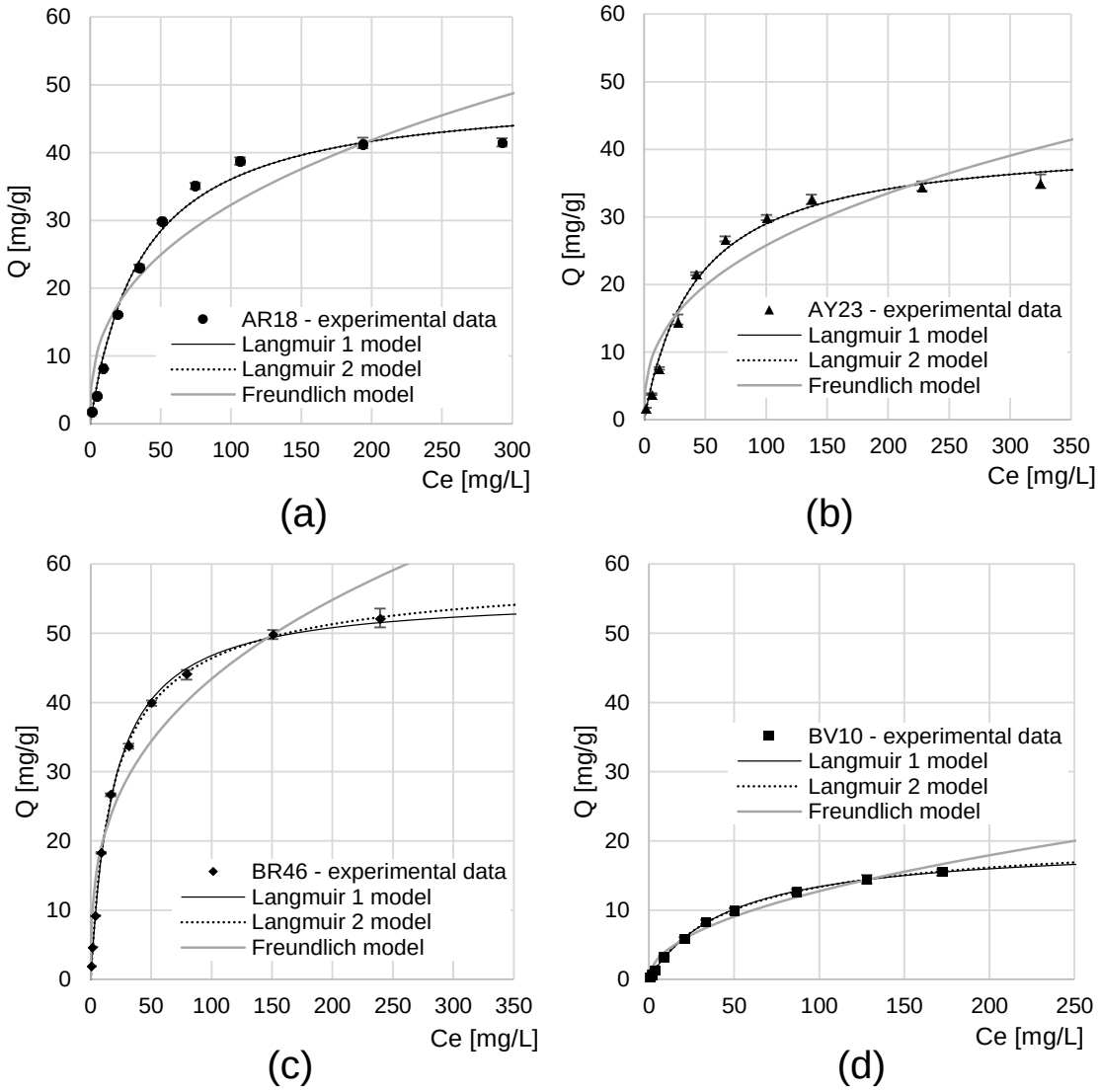

Figure 5. Isotherms of sorption of: (**a**) AR18, (**b**) AY23, (**c**) BR46, and (**d**) BV10 on RH (average + range). Langmuir 1,2, Freundlich models.

In the experimental series with AR18 and AY23, the K_1, K_2 and K_C constants determined from the Langmuir models 1 and 2 as well as the Q_{max} and R^2 reached the same numerical values (Table 4), which suggests that only one type of the sorption center played a major role in the sorption of acidic dyes onto RH. Presumably, this function was played by the protonated hydroxyl functional groups.

In the experimental series with BR46 and BV10, the Langmuir 2 model was found to describe experimental data better than the Langmuir 1 model, which suggests at least two different mechanisms of dye sorption onto RH. In the case of BR46, its sorption onto RH probably occurred through hydrogen bonds (between hydrogen and nitrogen atoms and between hydrogen and oxygen) and also through its ionic interaction with the ionized carboxyl groups. In contrast, the binding of BV10 on the tested sorbent, apart from hydrogen interactions, could also proceed via electrostatic interactions between the ionized carboxyl group of the dye and the protonated RH groups.

The maximum sorption capacities of RH towards AR18 and AY23 were quite similar and reached 49.37 and 41.52 mg/g, respectively. As mentioned earlier, the similar sorption effectiveness of these dyes may result from their similar particle sizes and the same number of acidic functional groups.

In turn, the maximum sorption capacities of the alkaline dyes were determined at 59.07 mg/g and 20.93 mg/g for BR46 and BV10, respectively. As mentioned in Section 3.3, the lower sorption capacity of the tested sorbent towards BV10 compared to BR46 was probably due to the acidic functional group (-COOH) being untypical for the basic dye, which generated the local negative charge. Two opposing charges in the BV10 structure significantly impaired the possibility of its sorption through electrostatic interactions with the sorbent's surface.

The higher sorption effectiveness of the basic dye BR46 onto RH compared to the acidic dyes AR18 and AY23 may be due to the generally acidic nature of the sorbent (pH_{PZC} = 6.62), which promotes the binding of cationic sorbates. The smaller size of the BR46 molecules also contributed to its better sorption effectiveness compared to AR18 and AY23, which allowed them to occupy active sites inaccessible to the acidic dyes.

The relatively small values of K_1 and K_2 constants (<0.5), determined from the Langmuir 2 model, confirm earlier findings suggesting the low affinity of the dyes to the active sites of RH. This finding indicates that the sorbent will be able to bind a large amount of dye only at high concentrations of the sorbate in the solution. In turn, the percentage removal effectiveness of dyes at their low concentrations will be relatively small in this case.

Table 5 lists the sorption capacities of various biosorbents and activated carbons towards the dyes analyzed in the present study.

Table 5. Sorption capacity of various biosorbents and activated carbons towards AR18, AY23, BR46, and BV10 dyes.

Dye	Sorbent	Sorption Capacity [mg/g]	pH of Sorption	Duration of Sorption [min]	References
AR18	Activated carbon WG-12	100	–	–	[55]
	Activated carbon from almond shell	51.6	2	60	[39]
	Rapeseed husks	49.4	2	150	This work
	Chitosan flakes	39.9	4	180	[38]
	Cellulose	29.7	6	120	[38]
	Activated Carbon from Poplar Wood	29.41	5	120	[48]
	Sargassum glaucescens biomass	15.0	6	60	[56]
	Agar	13.6	6	120	[38]
	Activated carbon from wood (polar tree)	3.9	7	120	[48]
	Sunflower seed hulls	1.8	3	90	[37]
	Coconut shells	0.66	2	45	[51]
AY23	Activated carbon from coconut coir	132.07	6	120	[49]
	Rapeseed husks	41.52	2	150	This work
	Chitin flakes	24.2	2	120	[41]
	Sawdust	4.7	3	70	[40]
	Sunflower seed hulls	2.3	3	90	[37]
	Coconut shell activated carbon	2.3	1.7	60	[57]
	Coconut shells	0.53	2	45	[51]
BR46	Granular activated carbon	333.3	8	<60	[44]
	Activated carbon from biomass	65.7	7	90	[58]
	Rapeseed husks	59.1	6	180	This work
	Spent green tea leaves	58	6	240	[45]
	Lemon peels	54	6	240	[42]
	Molts of mealworm	50.9	6	150	[46]
	Coconut shells	49.4	6	120	[51]
	Active carbon ROW 08	45	8	60	[59]
	Paulownia tomentosa tree leaves	43.1	8	72	[43]
	Exoskeletons of mealworm	31.5	6	180	[46]
	Nut sawdust	30.1	7	-	[60]
	Bone meal	24.6	6	90	[61]
	Wood sawdust	19.2	-	120	[50]

Table 5. *Cont.*

Dye	Sorbent	Sorption Capacity [mg/g]	pH of Sorption	Duration of Sorption [min]	References
BV10	Palm shell-based activated carbon	30	3	-	[47]
	Activated carbon from jute fiber	28	8	220	[62]
	Spent green tea leaves	26.7	3	240	[45]
	Rapeseed husks	20.9	3	180	This work
	Banana peels	20.6	7	1440	[63]
	Cedar cones	17.2	5	480	[64]
	Coconut fiber	14.9	9.2	90	[65]
	Sugar cane fiber	10.4	-	-	[66]
	Molts of mealworm	6.44	3	210	[46]
	Lemon peels	5.7	3	240	[42]
	Mango leaves (powder)	3.3	-	50	[67]
	Orange peels	3.2	4	-	[42]
	Coal-fired coconut fiber	2.6	6.5	150	[52]
	Powdered coffee	2.5	2	180	[53]

The sorption effectiveness of AR18 and AY23 dyes on the tested rapeseed husks is higher than on other investigated sorbents based on plant biomass, such as sawdust, seed husks or coconut shells (Table 5). Interestingly, the sorption capacity of RH towards the acidic dyes is higher than the sorption capacities of chitin sorbents and also certain activated carbons.

The sorption of BR46 and BV10 dyes onto RH is more effective than their sorption on most plant biomass sorbents, such as sawdust, leaves, nut shells or fruit skins (Table 5). As with acidic dyes, the sorption effectiveness of alkaline dyes onto RH is higher than of the selected activated carbon-based sorbents. RH is inferior only to commercial sorbents.

The high sorption capacity of RH towards both acidic and basic dyes suggests the possibility of using this unconventional sorbent as a cheaper alternative to the currently used commercial activated carbons. Since RH are characterized by lower sorption efficiency than commercial activated carbons, their actual dose used in water decolorization processes should be higher. A certain limitation of this biosorbent could also be its higher susceptibility to mechanical damage and the ability to putrefy compared to activated carbons. In addition, such a sorbent could be used only once because RH regeneration involving dye desorption would be rather cost-ineffective. Rapeseed husks used in the dye sorption process can be dried and co-combusted in heating plants or electrical power and heating stations, which will ensure energy recovery from the material. An alternative means of managing the spent sorbent from rapeseed husks may be to use it as a good raw material for the production of activated carbon, which can also be used for wastewater treatment.

4. Conclusions

Rapeseed husks can serve as a cheap sorbent for both anionic and cationic dyes. The maximum sorption capacity of RH towards AR18 and AY23 acidic dyes was 49.37 and 41.52 mg/g, respectively, while towards BR46 and BV10 basic dyes it reached 59.07 mg/g and 20.93 mg/g, respectively.

A prerequisite for achieving a high effectiveness of dye sorption onto RH is the appropriate pH of the solution during the process. The optimal pH for the sorption of AR18 and AY23 acidic dyes was established at pH = 2, whereas that of BR46 and BV10 basic dyes—at pH = 6 and pH = 3—respectively.

The pH of the solutions was observed to change during dye sorption onto rapeseed husks. The system always tended to achieve pH close to the pH $_{PZC}$ value of RH (pH_{PZC} = 6.62). The slightly acidic character of rapeseed husks is probably due to the higher ratio of carboxylic groups to amino groups on the sorbent's surface.

The time needed to reach the sorption equilibrium of dyes onto RH depended on their initial concentration and ranged from 120 to 150 min for the acidic dyes and from 150 to

180 min for the basic ones. Shorter sorption equilibrium times were achieved at higher concentrations of dyes, which is associated with a higher probability of dyes colliding with sorption sites and their faster saturation.

Data obtained from the Langmuir 1 and Langmuir 2 experimental models indicate that only one type of the sorption center, which is presumably the protonated amine groups, played the main role in AR18 and AY23 sorption onto RH. In turn, the binding of basic dyes onto RH took place via at least two different mechanisms. In the case of BR46, it presumably proceeded via hydrogen bonds as well as electrostatic interactions with the ionized carboxyl groups on the sorbent's surface. In the case of BV10, in addition to hydrogen bonds, the binding occurred through the ionic bonds between the carboxyl group of the dye and the protonated functional groups of RH.

Author Contributions: Conceptualization, T.J.; methodology, T.J.; software, T.J.; formal analysis, U.F.; investigation, T.J.; resources, T.J. and U.F.; data curation, T.J.; writing—original draft preparation, T.J.; writing—review and editing, U.F.; visualization, T.J.; supervision, T.J.; project administration, U.F.; funding acquisition, T.J. and U.F. All authors have read and agreed to the published version of the manuscript.

Funding: This study was financed under Project No. 29.610.023-110 of the University of Warmia and Mazury in Olsztyn, Poland.

Institutional Review Board Statement: Not applicable.

Informed Consent Statement: Not applicable.

Data Availability Statement: The data presented in this study are available on request from the corresponding author.

Conflicts of Interest: The authors declare no conflict of interest.

References

1. Wang, Z.; Park, H.N.; Won, S.W. Adsorption and Desorption Properties of Polyethylenimine/Polyvinyl Chloride Cross-Linked Fiber for the Treatment of Azo Dye Reactive Yellow 2. *Molecules* **2021**, *26*, 1519. [CrossRef]
2. Tejada-Tovar, C.; Villabona-Ortíz, Á.; Ortega-Toro, R. Removal of Metals and Dyes in Water Using Low-Cost Agro-Industrial Waste Materials. *Appl. Sci.* **2023**, *13*, 8481. [CrossRef]
3. Garg, A.; Chopra, L. Dye Waste: A Significant Environmental Hazard. *Mater. Today Proc.* **2022**, *48*, 1310–1315. [CrossRef]
4. Alsukaibi, A.K.D. Various Approaches for the Detoxification of Toxic Dyes in Wastewater. *Processes* **2022**, *10*, 1968. [CrossRef]
5. Sharma, J.; Sharma, S.; Soni, V. Classification and Impact of Synthetic Textile Dyes on Aquatic Flora: A Review. *Reg. Stud. Mar. Sci.* **2021**, *45*, 101802. [CrossRef]
6. Rápó, E.; Tonk, S. Factors Affecting Synthetic Dye Adsorption; Desorption Studies: A Review of Results from the Last Five Years (2017–2021). *Molecules* **2021**, *26*, 5419. [CrossRef] [PubMed]
7. Ouakouak, A.; Abdelhamid, M.; Thouraya, B.; Chahinez, H.O.; Hocine, G.; Hamdi, N.; Syafiuddin, A.; Boopathy, R. Development of a Novel Adsorbent Prepared from Dredging Sediment for Effective Removal of Dye in Aqueous Solutions. *Appl. Sci.* **2021**, *11*, 10722. [CrossRef]
8. Belda Marín, C.; Egles, C.; Landoulsi, J.; Guénin, E. Silk Bionanocomposites for Organic Dye Absorption and Degradation. *Appl. Sci.* **2022**, *12*, 9152. [CrossRef]
9. Rane, A.; Joshi, S.J. Biodecolorization and Biodegradation of Dyes: A Review. *Open Biotechnol. J.* **2021**, *15*, 97–108. [CrossRef]
10. Pimentel, C.H.; Freire, M.S.; Gómez-Díaz, D.; González-Álvarez, J. Removal of Wood Dyes from Aqueous Solutions by Sorption on Untreated Pine (*Pinus radiata*) Sawdust. *Cellulose* **2023**, *30*, 4587–4608. [CrossRef]
11. Bilal, M.; Ihsanullah, I.; Hassan Shah, M.U.; Bhaskar Reddy, A.V.; Aminabhavi, T.M. Recent Advances in the Removal of Dyes from Wastewater Using Low-Cost Adsorbents. *J. Environ. Manag.* **2022**, *321*, 115981. [CrossRef]
12. Husien, S.; El-taweel, R.M.; Salim, A.I.; Fahim, I.S.; Said, L.A.; Radwan, A.G. Review of Activated Carbon Adsorbent Material for Textile Dyes Removal: Preparation, and Modelling. *Curr. Res. Green Sustain. Chem.* **2022**, *5*, 100325. [CrossRef]
13. Bhat, S.; Uthappa, U.T.; Sadhasivam, T.; Altalhi, T.; Soo Han, S.; Kurkuri, M.D. Abundant Cilantro Derived High Surface Area Activated Carbon (AC) for Superior Adsorption Performances of Cationic/Anionic Dyes and Supercapacitor Application. *Chem. Eng. J.* **2023**, *459*, 141577. [CrossRef]
14. Farhadi, A.; Ameri, A.; Tamjidi, S. Application of Agricultural Wastes as a Low-Cost Adsorbent for Removal of Heavy Metals and Dyes from Wastewater: A Review Study. *Phys. Chem. Res.* **2021**, *9*, 211–226. [CrossRef]
15. Sulyman, M.; Namiesnik, J.; Gierak, A. Low-Cost Adsorbents Derived from Agricultural By-Products/Wastes for Enhancing Contaminant from Wastewater: A Review. *Pol. J. Environ. Stud.* **2017**, *26*, 479–510. [CrossRef]

16. Cretescu, I.; Lupascu, T.; Buciscanu, I.; Balau-Mindru, T.; Soreanu, G. Low-Cost Sorbents for the Removal of Acid Dyes from Aqueous Solutions. *Process Saf. Environ. Prot.* **2017**, *108*, 57–66. [CrossRef]
17. Ahmed, F.S.; Abdul Razak, A.A.; Muslim, M.A. The Use of Inexpensive Sorbents to Remove Dyes from Wastewater—A Review. *Eng. Technol. J.* **2022**, *40*, 498–515. [CrossRef]
18. Raboanatahiry, N.; Li, H.; Yu, L.; Li, M. Rapeseed (*Brassica napus*): Processing, Utilization, and Genetic Improvement. *Agronomy* **2021**, *11*, 1776. [CrossRef]
19. Jafarian Asl, P.; Niazmand, R. Bioactive Phytochemicals from Rapeseed (*Brassica napus*) Oil Processing By-Products. In *Reference Series in Phytochemistry*; Springer: Berlin/Heidelberg, Germany, 2023; pp. 27–47.
20. Cartea, E.; De Haro-Bailón, A.; Padilla, G.; Obregón-Cano, S.; Del Rio-Celestino, M.; Ordás, A. Seed Oil Quality of *Brassica napus* and *Brassica rapa* Germplasm from Northwestern Spain. *Foods* **2019**, *8*, 292. [CrossRef] [PubMed]
21. Hazrat, M.A.; Rasul, M.G.; Khan, M.M.K.; Ashwath, N.; Fattah, I.M.R.; Ong, H.C.; Mahlia, T.M.I. Biodiesel Production from Transesterification of Australian *Brassica napus* L. Oil: Optimisation and Reaction Kinetic Model Development. *Environ. Dev. Sustain.* **2023**, *25*, 12247–12272. [CrossRef]
22. Carré, P.; Quinsac, A.; Citeau, M.; Fine, F. A Re-Examination of the Technical Feasibility and Economic Viability of Rapeseed Dehulling. *OCL—Oilseeds Fats* **2015**, *22*, D304. [CrossRef]
23. Boucher, J.; Chabloz, C.; Lex, O.; Marison, I.W. Oleaginous Seeds, Press-Cake and Seed Husks for the Biosorption of Metals. *J. Water Supply Res. Technol.—AQUA* **2008**, *57*, 489–499. [CrossRef]
24. Carre, P.; Citeau, M.; Robin, G.; Estorges, M. Hull Content and Chemical Composition of Whole Seeds, Hulls and Germs in Cultivars of Rapeseed (*Brassica napus*). *OCL* **2016**, *23*, A302. [CrossRef]
25. VanDer Kamp, K.A.; Qiang, D.; Aburub, A.; Wurster, D.E. Modified Langmuir-like Model for Modeling the Adsorption from Aqueous Solutions by Activated Carbons. *Langmuir* **2005**, *21*, 217–224. [CrossRef] [PubMed]
26. Rehman, Z.U.; Vrouwenvelder, J.S.; Saikaly, P.E. Physicochemical Properties of Extracellular Polymeric Substances Produced by Three Bacterial Isolates from Biofouled Reverse Osmosis Membranes. *Front. Microbiol.* **2021**, *12*, 668761. [CrossRef]
27. Nandiyanto, A.B.D.; Oktiani, R.; Ragadhita, R. How to Read and Interpret Ftir Spectroscope of Organic Material. *Indones. J. Sci. Technol.* **2019**, *4*, 97–118. [CrossRef]
28. Sulieman, A.A.; Zhu, K.X.; Peng, W.; Hassan, H.A.; Obadi, M.; Ahmed, M.I.; Zhou, H.M. Effect of *Agaricus bisporus* Polysaccharide Flour and Inulin on the Antioxidant and Structural Properties of Gluten-Free Breads. *J. Food Meas. Charact.* **2019**, *13*, 1884–1897. [CrossRef]
29. Hospodarova, V.; Singovszka, E.; Stevulova, N. Characterization of Cellulosic Fibers by FTIR Spectroscopy for Their Further Implementation to Building Materials. *Am. J. Anal. Chem.* **2018**, *09*, 303–310. [CrossRef]
30. Rana, R.; Langenfeld-Heyser, R.; Finkeldey, R.; Polle, A. FTIR Spectroscopy, Chemical and Histochemical Characterisation of Wood and Lignin of Five Tropical Timber Wood Species of the Family of Dipterocarpaceae. *Wood Sci. Technol.* **2010**, *44*, 225–242. [CrossRef]
31. Stępień, E.; Kamińska, A.; Surman, M.; Karbowska, D.; Wróbel, A.; Przybyło, M. Fourier-Transform InfraRed (FT-IR) Spectroscopy to Show Alterations in Molecular Composition of EV Subpopulations from Melanoma Cell Lines in Different Malignancy. *Biochem. Biophys. Rep.* **2021**, *25*, 100888. [CrossRef]
32. Kukula-Koch, W.; Grzybek, M.; Strachecka, A.; Jaworska, A.; Ludwiczuk, A. ATR-FTIR-Based Fingerprinting of Some Cucurbitaceae Extracts: A Preliminary Study. *Acta Soc. Bot. Pol.* **2018**, *87*. [CrossRef]
33. Ch'ng, H.Y.; Ahmed, O.H.; Majid, N.M.A. Qualitative Assessment of Soil Carbon in a Rehabilitated Forest Using Fourier Transform Infrared Spectroscopy. *Sci. World J.* **2011**, *11*, 532–545. [CrossRef]
34. Multescu, M.; Marinas, I.C.; Susman, I.E.; Belc, N. Byproducts (Flour, Meals, and Groats) from the Vegetable Oil Industry as a Potential Source of Antioxidants. *Foods* **2022**, *11*, 253. [CrossRef]
35. Sivakumar, S.; Khatiwada, C.P.; Sivasubramanian, J.; Jini, P.; Prabu, N.; Venkateson, A.; Soundararajan, P. FT-IR Study of Green Tea Leaves and Their Diseases of Arunachal Pradesh, North East, India. *Afr. J. Parasitol. Res.* **2013**, *3*, 166–172.
36. Navarro, R.; Guzmán, J.; Saucedo, I.; Revilla, J.; Guibal, E. Recovery of Metal Ions by Chitosan: Sorption Mechanisms and Influence of Metal Speciation. *Macromol. Biosci.* **2003**, *3*, 552–561. [CrossRef]
37. Jóźwiak, T.; Filipkowska, U.; Brym, S.; Kopeć, L. Use of Aminated Hulls of Sunflower Seeds for the Removal of Anionic Dyes from Aqueous Solutions. *Int. J. Environ. Sci. Technol.* **2020**, *17*, 1211–1224. [CrossRef]
38. Kuczajowska-Zadrożna, M.; Filipkowska, U.; Jóźwiak, T.; Szymczyk, P. The Use of Polysaccharides for Acid Red 18 Anionic Dye Removal from Aqueous Solutions. *Prog. Chem. Appl. Chitin Deriv.* **2017**, *22*, 106–117. [CrossRef]
39. Chaleshtori, A.N.; Meghadddam, F.M.; Sadeghi, M.M.; Rahimi, R.R.; Hemati, S.; Ahmadi, A. Removal of Acid Red 18 (Azo-Dye) from Aqueous Solution by Adsorption onto Activated Charcoal Prepared from Almond Shell. *J. Environ. Sci. Manag.* **2017**, *20*, 9–16. [CrossRef]
40. Banerjee, S.; Chattopadhyaya, M.C. Adsorption Characteristics for the Removal of a Toxic Dye, Tartrazine from Aqueous Solutions by a Low Cost Agricultural by-Product. *Arab. J. Chem.* **2017**, *10*, S1629–S1638. [CrossRef]
41. Filipkowska, U.; Kuczajowska-Zadrożna, M.; Jóźwiak, T.; Szymczyk, P.; Kaczyński, A. Adsorption of Basic Yellow 28 (BY 28) and Acid Yellow 23 (AY 23) Dyes onto Chitin. *Prog. Chem. Appl. Chitin Deriv.* **2015**, *20*, 34–42. [CrossRef]
42. Jóźwiak, T.; Filipkowska, U.; Zajko, P. Use of Citrus Fruit Peels (Grapefruit, Mandarin, Orange, and Lemon) as Sorbents for the Removal of Basic Violet 10 and Basic Red 46 from Aqueous Solutions. *Desalination Water Treat.* **2019**, *163*, 385–397. [CrossRef]

43. Deniz, F.; Saygideger, S.D. Removal of a Hazardous Azo Dye (Basic Red 46) from Aqueous Solution by Princess Tree Leaf. *Desalination* **2011**, *268*, 6–11. [CrossRef]
44. Abdul Halim, H.N.; Mee, K.L.K. Adsorption of Basic Red 46 by Granular Activated Carbon in a Fixed- Bed Column. *Int. Conf. Environ. Ind. Innov.* **2011**, *12*, 263–267.
45. Jóźwiak, T.; Filipkowska, U.; Struk-Sokołowska, J.; Bryszewski, K.; Trzciński, K.; Kuźma, J.; Ślimkowska, M. The Use of Spent Coffee Grounds and Spent Green Tea Leaves for the Removal of Cationic Dyes from Aqueous Solutions. *Sci. Rep.* **2021**, *11*, 9584. [CrossRef]
46. Kurowska, P.; Jóźwiak, T.; Filipkowska, U.; Bakuła, T. The use of chitin in the moults and exoskeletons of mealworms (*Tenebrio molitor*) to remove cationic dyes from aqueous solutions. *Prog. Chem. Appl. Chitin Deriv.* **2023**, *28*, 56–74. [CrossRef]
47. Mohammadi, M.; Hassani, A.J.; Mohamed, A.R.; Najafpour, G.D. Removal of Rhodamine b from Aqueous Solution Using Palm Shell-Based Activated Carbon: Adsorption and Kinetic Studies. *J. Chem. Eng. Data* **2010**, *55*, 5777–5785. [CrossRef]
48. Shokoohi, R.; Vatanpoor, V.; Zarrabi, M.; Vatani, A. Adsorption of Acid Red 18 (AR18) by Activated Carbon from Poplar Wood—A Kinetic and Equilibrium Study. *J. Chem.* **2010**, *7*, 65–72. [CrossRef]
49. de Souza Macedo, J.; da Costa Júnior, N.B.; Almeida, L.E.; da Silva Vieira, E.F.; Cestari, A.R.; de Fátima Gimenez, I.; Villarreal Carreño, N.L.; Barreto, L.S. Kinetic and Calorimetric Study of the Adsorption of Dyes on Mesoporous Activated Carbon Prepared from Coconut Coir Dust. *J. Colloid Interface Sci.* **2006**, *298*, 515–522. [CrossRef]
50. Laasri, L.; Elamrani, M.K.; Cherkaoui, O. Removal of Two Cationic Dyes from a Textile Effluent by Filtration-Adsorption on Wood Sawdust. *Environ. Sci. Pollut. Res.* **2007**, *14*, 237–240. [CrossRef] [PubMed]
51. Józwiak, T.; Filipkowska, U.; Bugajska, P.; Kalkowski, T. The Use of Coconut Shells for the Removal of Dyes from Aqueous Solutions. *J. Ecol. Eng.* **2018**, *19*, 129–135. [CrossRef]
52. Namasivayam, C.; Dinesh Kumar, M.; Selvi, K.; Ashruffunissa Begum, R.; Vanathi, T.; Yamuna, R.T. "Waste" Coir Pith—A Potential Biomass for the Treatment of Dyeing Wastewaters. *Biomass Bioenergy* **2001**, *21*, 477–483. [CrossRef]
53. Shen, K.; Gondal, M.A. Removal of Hazardous Rhodamine Dye from Water by Adsorption onto Exhausted Coffee Ground. *J. Saudi Chem. Soc.* **2017**, *21*, S120–S127. [CrossRef]
54. Cheng, C.S.; Deng, J.; Lei, B.; He, A.; Zhang, X.; Ma, L.; Li, S.; Zhao, C. Toward 3D Graphene Oxide Gels Based Adsorbents for High-Efficient Water Treatment via the Promotion of Biopolymers. *J. Hazard. Mater.* **2013**, *263*, 467–478. [CrossRef]
55. Okoniewska, E. Removal of the Dye of Acid Bright Red 4R from Water Solutions on Activated Carbons. *Eng. Prot. Environ.* **2016**, *19*, 331–340. [CrossRef]
56. Zazouli, M.A.; Moradi, E.; Zazouli, M.A.; Moradi, E. Adsorption Acid Red18 Dye Using Sargassum Glaucescens Biomass from Aqueous Solutions. *Iran. J. Health Sci.* **2015**, *3*, 7–13. [CrossRef]
57. Jibril, M.; Noraini, J.; Poh, L.S.; Mohammed Evuti, A. Removal of Colour from Waste Water Using Coconut Shell Activated Carbon (CSAC) and Commercial Activated Carbon (CAC). *J. Teknol.* **2012**, *60*, 15–19. [CrossRef]
58. Azmi, N.A.I.; Zainudin, N.F.; Ali, U.F.M. Adsorption of Basic Red 46 Using Sea Mango (*Cerbera odollam*) Based Activated Carbon. *AIP Conf. Proc.* **2015**, *1660*, 070068. [CrossRef]
59. Madeła, M.; Krzemińska, D.; Neczaj, E. Wpływ Procesu Fentona Na Skuteczność Usuwania Zanieczyszczeń Ze Ścieków Przemysłowych Na Węglach Aktywnych. *Technol. Wody* **2014**, *5*, 46–50.
60. Yeddou, N.; Bensmaili, A. Kinetic Models for the Sorption of Dye from Aqueous Solution by Clay-Wood Sawdust Mixture. *Desalination* **2005**, *185*, 499–508. [CrossRef]
61. EL Haddad, M.; Rachid, M.; Slimani, R.; Nabil, S.; Ridaoui, M.; Lazar, S. Adsorptive removal of a cationic dye—Basic red 46—From aqueous solutions using animal bone meal. *J. Eng. Stud. Res.* **2012**, *18*, 43.
62. Porkodi, K.; Vasanth Kumar, K. Equilibrium, Kinetics and Mechanism Modeling and Simulation of Basic and Acid Dyes Sorption onto Jute Fiber Carbon: Eosin Yellow, Malachite Green and Crystal Violet Single Component Systems. *J. Hazard. Mater.* **2007**, *143*, 311–327. [CrossRef] [PubMed]
63. Annadurai, G.; Juang, R.S.; Lee, D.J. Use of Cellulose-Based Wastes for Adsorption of Dyes from Aqueous Solutions. *J. Hazard. Mater.* **2002**, *92*, 263–274. [CrossRef] [PubMed]
64. Zamouche, M.; Hamdaoui, O. Sorption of Rhodamine B by Cedar Cone: Effect of PH and Ionic Strength. *Energy Procedia* **2012**, *18*, 1228–1239. [CrossRef]
65. Sureshkumar, M.V.; Namasivayam, C. Adsorption Behavior of Direct Red 12B and Rhodamine B from Water onto Surfactant-Modified Coconut Coir Pith. *Colloids Surf. A Physicochem. Eng. Asp.* **2008**, *317*, 277–283. [CrossRef]
66. Parab, H.; Sudersanan, M.; Shenoy, N.; Pathare, T.; Vaze, B. Use of Agro-Industrial Wastes for Removal of Basic Dyes from Aqueous Solutions. *Clean* **2009**, *37*, 963–969. [CrossRef]
67. Khan, T.A.; Sharma, S.; Ali, I. Adsorption of Rhodamine B Dye from Aqueous Solution onto Acid Activated Mango (*Magnifera indica*) Leaf Powder: Equilibrium, Kinetic and Thermodynamic Studies. *J. Toxicol. Environ. Health Sci.* **2011**, *3*, 286–297.